In Vivo Biodistribution and Small Animal PET of ^{64}Cu-Labeled Antimicrobial Peptoids

Jiwon Seo,[#,§] Gang Ren,[#,†] Hongguang Liu,[†] Zheng Miao,[†] Minyoung Park,[⊥] Yihong Wang,[†] Tyler M. Miller,[‡] Annelise E. Barron,*[,‡] and Zhen Cheng*[,†]

[†]Molecular Imaging Program at Stanford (MIPS), Department of Radiology, Bio-X Program, Canary Center at Stanford for Cancer Early Detection, Stanford University, California, 94305-5344, United States

[‡]Department of Bioengineering, [⊥]Department of Chemical and Systems Biology, Stanford University, California, 94305-5440, United States

[§]School of General Studies, Gwangju Institute of Science and Technology, Gwangju 500-712, Republic of Korea

Ⓢ *Supporting Information*

ABSTRACT: Peptoids are a rapidly developing class of biomimetic polymers based on oligo-*N*-substituted glycine backbones, designed to mimic peptides and proteins. Inspired by natural antimicrobial peptides, a group of cationic amphipathic peptoids has been successfully discovered with potent, broad-spectrum activity against pathogenic bacteria; however, there are limited studies to address the *in vivo* pharmacokinetics of the peptoids. Herein, ^{64}Cu-labeled DOTA conjugates of three different peptoids and two control peptides were synthesized and assayed *in vivo* by both biodistribution studies and small animal positron emission tomography (PET). The study was designed in a way to assess how structural differences of the peptidomimetics affect *in vivo* pharmacokinetics. As amphipathic molecules, major uptake of the peptoids occurred in the liver. Increased kidney uptake was observed by deleting one hydrophobic residue in the peptoid, and [64]**Cu-3** achieved the highest kidney uptake of all the conjugates tested in this study. In comparison to peptides, our data indicated that peptoids had general *in vivo* properties of higher tissue accumulation, slower elimination, and higher *in vivo* stability. Different administration routes (intravenous, intraperitoneal, and oral) were investigated with peptoids. When administered orally, the peptoids showed poor bioavailability, reminiscent of that of peptide. However, remarkably longer passage through the gastrointestinal (GI) tract without rapid digestion was observed for peptoids. These unique *in vivo* properties of peptoids were rationalized by efficient cellular membrane permeability and protease resistance of peptoids. The results observed in the biodistribution studies could be confirmed by PET imaging, which provides a reliable way to evaluate *in vivo* pharmacokinetic properties of peptoids noninvasively and in real time. The pharmacokinetic data presented here can provide insight for further development of the antimicrobial peptoids as pharmaceuticals.
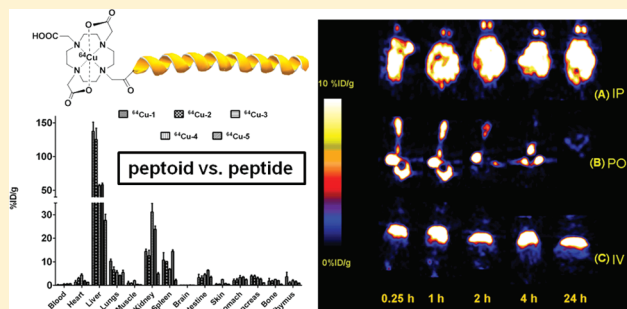
■ INTRODUCTION

Over recent decades, a number of antimicrobial peptides (AMPs) have been identified as a front-line defense in various host organisms.[1,2] AMPs have drawn great scientific interest because they not only belong to the intrinsic host-defense system,[3–6] but also are promising candidates for the development of novel anti-infective agents.[7,8] Natural AMP-based therapeutics demonstrate activities against broad-spectrum pathogens *in vitro*; however, they exhibit major drawbacks *in vivo* such as their low resistance against proteolysis and rapid clearance by the kidneys.[9,10] Recently, the challenges associated with peptides are being addressed owing to the use of non-natural amino acids and modified peptide structures;[11,12] hence, various peptidomimetics that are designed to reproduce critical AMP structural characteristics, such as spatially segregated cationicity and hydrophobicity in an amphipathic secondary structure, have been developed.[13–18]

Particularly, short (<40 amino acids), cationic, linear, and α-helical AMPs are amenable to mimicry, and peptoids are among the front-runners in mimicking this class of AMPs.

Peptoids (oligo-*N*-substituted glycines) are a novel class of peptidomimetics that differ from peptides only in that side chains are attached to the backbone amide nitrogen instead of the α-carbon (Figure 1).[19,20] This unique structural feature of peptoids leads to quite different pharmacological properties from natural peptides: (1) they are highly stable against proteases;[21,22] (2) they lack hydrogen-bonding potential, which further prevents backbone-driven aggregation and thus increases bioavailability;[23,24] (3) they show increased cell permeability over

A

B

Peptide

Peptoid

Nspe
(S)-N-(1-phenylethyl)glycine

NLys
N-(4-aminobutyl)glycine

Npm
N-(phenylmethyl)glycine

DOTA

C

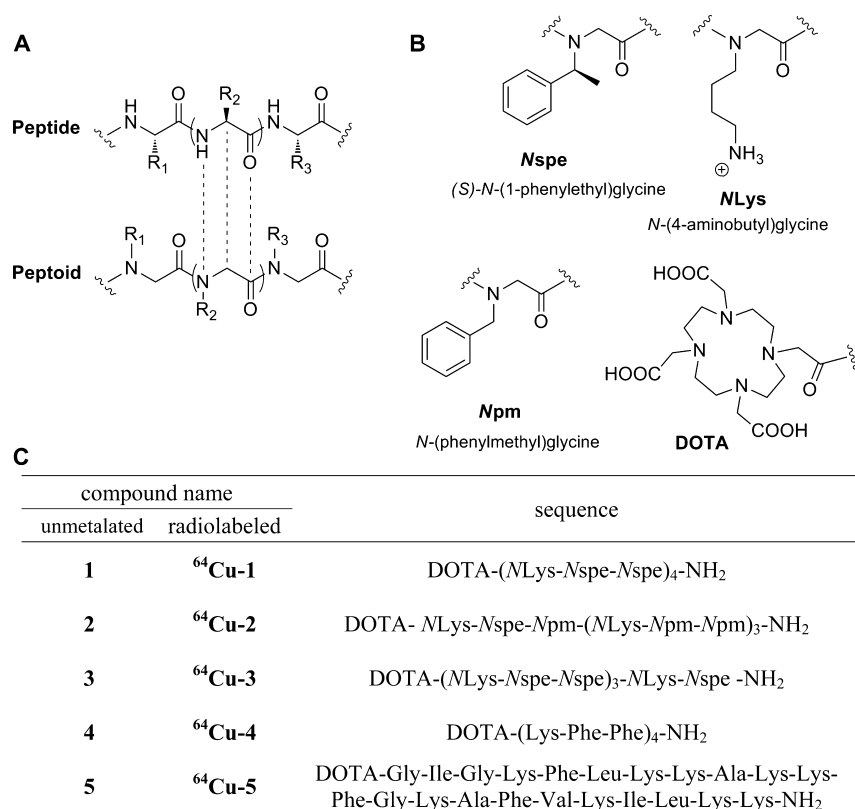| compound name		sequence
unmetalated	radiolabeled	
1	[64]Cu-**1**	DOTA-(NLys-Nspe-Nspe)$_4$-NH$_2$
2	[64]Cu-**2**	DOTA- NLys-Nspe-Npm-(NLys-Npm-Npm)$_3$-NH$_2$
3	[64]Cu-**3**	DOTA-(NLys-Nspe-Nspe)$_3$-NLys-Nspe -NH$_2$
4	[64]Cu-**4**	DOTA-(Lys-Phe-Phe)$_4$-NH$_2$
5	[64]Cu-**5**	DOTA-Gly-Ile-Gly-Lys-Phe-Leu-Lys-Lys-Ala-Lys-Lys-Phe-Gly-Lys-Ala-Phe-Val-Lys-Ile-Leu-Lys-Lys-NH$_2$

Figure 1. (A) Comparison of peptide and peptoid. (B) Chemical structures of peptoid submonomers and DOTA. (C) Sequences of the synthesized DOTA conjugates and corresponding compound names.

peptides;[23,25] and (4) they may evade immune recognition.[26] Peptoids can be readily synthesized using a conventional solid-phase peptide synthesis (SPPS) method, and diverse sequences of peptoids can be prepared at relatively low cost. They are also precisely tunable in conjugation with established synthetic methods.[27] Since their development in the early 1990s, peptoids have become attractive scaffolds for many different biological applications.[28−30] For example, the use of peptoids as antimicrobial agents,[31−36] molecular transporters for intracellular drug delivery,[37] or ligands for tumor receptor binding has been reported.[25]

Among many peptidomimetic systems under study, peptoids are particularly well suited for structural mimicry of AMPs[31,32] because they can readily form helical secondary structures via a periodic incorporation of bulky, α-chiral side chains.[38−40] The structures of the peptoid helices have been characterized to be stable polyproline type-I-like helices which exhibit a pitch of 6.0−6.7 Å and a periodicity of approximately three residues per turn.[41−43] The threefold periodicity of the peptoid helix makes it easier to mimic the facially amphipathic structures similar to those found in many AMPs; for example, the trimer repeat (X-Y-Z)$_n$ forms a peptoid helix with three faces, composed of X, Y, and Z residues. Previously, a group of cationic amphipathic peptoids, with broad-spectrum antimicrobial activity against both Gram-positive and Gram-negative bacteria including clinically relevant biosafety level 2 (BSL-2) pathogens, has been discovered.[31−34] Interestingly, these antimicrobial peptoids also show potential in treating multidrug resistant strains such as *Pseudomonas aeruginosa* biofilms[35] and *Micobacterium tuberculosis*.[36] Furthermore, we recently found that the cationic amphipathic peptoids were potent against several cancer cell lines at low micromolar concentrations, and their actions were

not affected by multidrug resistance (MDR) developed in cancer cells.[44] Therefore, cationic amphipathic peptoids represent an excellent molecular platform for the development of antimicrobials as well as cytotoxic chemotherapeutics and warrant systematic investigations on their *in vivo* behaviors.

The *in vivo* pharmacokinetic studies on antimicrobial peptides have been reported using radiolabeled peptides;[45,46] however, we cannot simply extrapolate peptoid biodistribution from previous peptide biodistribution data. First, due to the lack of hydrogen-bond donors in the peptoid backbone, the hydrodynamic radii of peptides and peptoids are expected to be significantly different.[24] Second, peptoids are protease-resistant and metabolically more stable than peptides.[21,22] For these reasons, the pharmacokinetic profiles of peptoids are likely to be different from what was observed with peptides, and a new set of pharmacokinetic data are required for better understanding the *in vivo* behavior of this unique family of peptidomimetics.

Recently, we found that antimicrobial peptoids showed different *in vitro* antimicrobial activity depending on their degree of helicity, chain length, and hydrophobicity (Table 1; note that the biological data are for oligomers without DOTA conjugation). Then, we reasoned that the different structural and physicochemical properties could also cause distinct *in vivo* pharmacokinetic profiles of the peptoids. Herein, three cationic amphipathic peptoids and two control peptides were selected, and their *in vivo* profiles were evaluated using both biodistribution and small animal positron emission tomography (PET). Peptoids **1**, **2**, and **3** represent N-terminal 1,4,7,10-tetraazacyclododecane-1,4,7,10-tetraacetic acid (DOTA) conjugates of cationic amphipathic peptides (Table 1 and Figure 1). Peptoids **1** and **3**, where the latter is almost identical to **1** except that it has one less C-terminal Nspe monomer, are linear peptoid

Table 1. Properties of 1−5

compounds	class	chain length[a]	secondary structure[b]	hydrophobicity (t_R in minutes)[d]	antimicrobial activity[e]	
					E. coli MIC, μM	selectivity ratio[f]
1	peptoid	12	helical	25.0	3.5−6.3	6.0
2	peptoid	12	almost unstructured	24.1	6.3	205
3	peptoid	11	helical	23.9	6.3	132
4	peptide	12	helix-like	24.0	ND	ND
5	peptide	22	random coil[c]	21.3	3.1−6.3	24

[a]Number of peptoid or peptide residues. [b]Determined by circular dichroism spectroscopy. [c]Fold into helical conformation upon binding to lipid membranes.[47,48] [d]Detailed HPLC conditions are provided in the Experimental Procedure section. HPLC chromatograms are shown in the Supporting Information (t_R: retention time in reverse phase HPLC column). [e]Biological data are for peptoids or peptides without DOTA conjugation. MIC (minimum inhibitory concentration) values and selectivity ratios for **1** and **5** are from ref 32, and for **2** and **3** are unpublished results. [f]Selectivity ratio = $(HD_{10})/(E.\ coli\ MIC)$. HD_{10}: 10% hemolytic dose.

helices. Peptoid **3** (without DOTA) has lower hydrophobicity than peptoid **1** (without DOTA) and was recently found to have substantially higher selectivity in killing bacterial cells without significant loss in potency (Table 1). Peptoid **2** (without DOTA) is a nonstructured peptoid, which nonetheless can adopt a helical conformation in the presence of the anionic bacterial membrane that serves as an organizing surface. For comparison, we tested two cationic amphipathic peptide controls: (1) peptide **4** has a direct sequence homology to peptoid **1**, and the effect of the peptoid backbone versus the peptide backbone was examined; and (2) peptide **5** is based on a well-known antimicrobial peptide, namely, pexiganan,[47,48] which advanced to phase 3 clinical trials.[49] Also known as MSI-78, pexiganan exhibits a random coil conformation, which folds into a helical conformation upon binding to a bacterial membrane (Table 1). To obtain kinetic data for the biodistribution and clearance for 24 h, a radionuclide with an appropriate half-life was needed. Therefore, DOTA-chelated ^{64}Cu was used due to its relatively long half-life (762 min) and numerous precedent biodistribution data of the DOTA-^{64}Cu labeled peptides.[50−52] With the radiolabeled peptoids and peptides, three different administration routes (intravenous, intraperitoneal, and oral) were examined. The results reported here can provide insight for future development of peptoids as antimicrobial chemotherapeutics.

■ EXPERIMENTAL PROCEDURES

Materials. All reagents were purchased from Sigma-Aldrich, Fisher, and Novabiochem. They were used without further purification unless stated otherwise. DOTA-tris(*t*-Bu ester) (or tri-*tert*-butyl 1,4,7,10-tetraazacyclododecane-1,4,7,10-tetraacetate) was purchased from Macrocyclics, TX, USA. *N,N*′-Diisopropyl-carbodiimide was purchased from Advanced ChemTech, KY, USA. Radioisotope ^{64}Cu was purchased from the Department of Medical Physics, University of Wisconsin, Madison, WI, USA. Six-week-old Balb/c mice were ordered from Harlan, CA, USA.

Synthesis and Purification. The peptoid oligomers were synthesized by solid-phase submonomer method using an automated peptide synthesizer (ABI 433A, Applied Biosystems, CA, USA).[20,53] Rink amide resin (0.60 mmol/g, Novabiochem, San Diego, CA) was used to generate C-terminal amide peptides. After Fmoc deprotection, each monomer was added by a series of bromoacetylation and displacement by an amine. These two steps were iterated with appropriate amines until the desired peptoid sequence was obtained. Typically, 0.06 mmol reaction scale was used (0.1 g of the resin). For bromoacetylation, the addition of bromoacetic acid (1 mL, 1.2 M in *N,N*-dimethylformamide (DMF), 1.2 mmol) followed by *N,N*′-diisopropylcarbodiimide (0.15 mL, neat, 1.0 mmol), and then agitation at room

temperature for 20 min were performed. For the displacement reaction, primary amine (1 mL, 1.5 M in *N*-methylpyrrolidone (NMP), 1.5 mmol) was added, and the reactor was agitated at room temperature for 1 h. The resin was washed with DMF (6 mL × 5) between each step. Peptide oligomers were prepared by the automated solid-phase peptide synthesis according to standard Fmoc/tBu-methodology and HBTU/HOBt/DIEA coupling.[54] Rink amide resin (0.60 mmol/g) was used to obtain C-terminal amide peptides. After completion of the solid-phase synthesis, the DOTA chelator was manually conjugated at the N-terminus of the pepoids or peptides by activating the carboxylic acid of DOTA-tris(*t*-Bu ester) with HATU. Peptoid (or peptide) attached on resin (properly protected, 0.025 mmol) was swelled in DMF (2 mL). To this was added DOTA-tris(*t*-Bu ester) (0.15 mmol), 2-(7-aza-1*H*-benzotriazole-1-yl)-1,1,3,3-tetramethyluronium hexafluoro-phosphate (HATU) (0.30 mmol), and *N,N*-diisopropylethyl-amine (DIPEA) (0.75 mmol), and the reaction continued at room temperature overnight.[55] Cleavage from the resin and deprotection were performed with 95:2.5:2.5 TFA/water/triisopropylsilane (v/v/v) for 2−3 h at room temperature. It should be noted that shorter cleavage time resulted in incomplete *tert*-butyl ester deprotection of DOTA-tris(*t*-Bu ester). The cleavage solution was filtered by solid-phase extraction (SPE) cartridges (Applied Separations, Allentown, PA, USA) and the volatiles were removed by a stream of nitrogen. The crude peptoid was dissolved in acetonitrile/water, lyophilized, and ana-lyzed by ESI-MS (or MALDI-TOF) and analytical HPLC.

Analytical HPLC was performed on a Waters 2695 separations module system with Waters 2998 photodiode array detector and Waters Alliance column heater. Phenomenex Jupiter C18 (250 × 2.0 mm, 5 μ, 300 Å) column was used for the analytical HPLC and the column was heated at 55 °C. Sample purity was monitored by absorbance at 220 nm. The mobile phase was used as follows: [A, water + 0.1% trifluoroacetic acid (TFA); B, CH_3CN + 0.1% TFA] 3 min using 1% B, then a linear gradient to 99% B over 30 min, a linear gradient back to 1% B over 10 min, and then 2 min using 1% B. Flow rate of the analytical HPLC was 0.2 mL/min.

The peptoids or peptides were purified by a preparative HPLC system (Waters PrepLC system, Waters 2489 UV/Visible detector, Waters fraction collector III) using a C18 column (Phenomenex Jupiter C18, 250 × 21.20 mm, 10 μm, 300 Å) at a flow rate of 25 mL/min. Sample elution was detected by absorbance at 220 and 260 nm. The purity of the product frac-tions was confirmed by analytical HPLC, and fractions containing pure product (>98% purity) were collected, lyophilized, and stored at −80 °C.
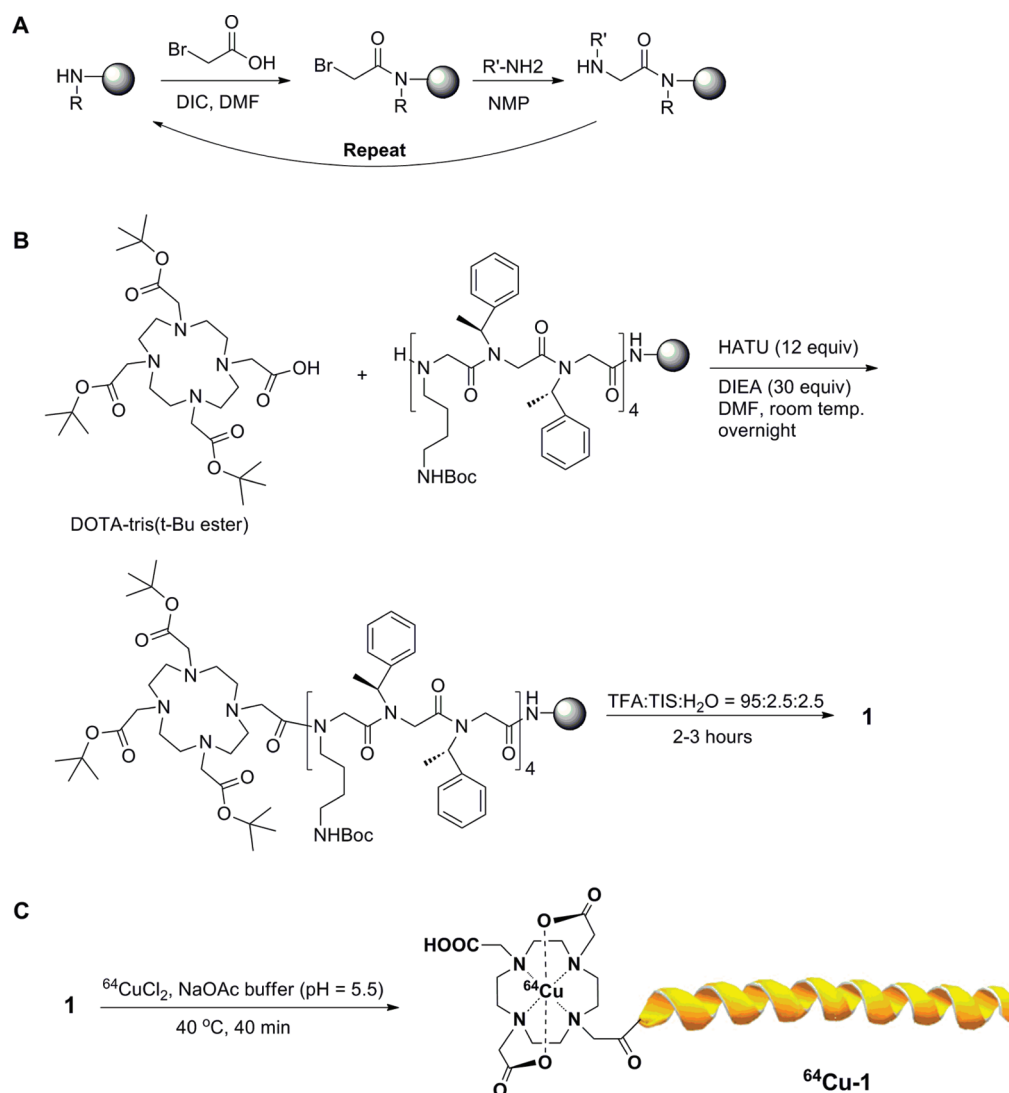
Figure 2. (A) Peptoid submonomer synthesis protocol. (B) Representative synthetic scheme of DOTA conjugates. (C) Illustrative structure of ^{64}Cu-1 prepared by ^{64}Cu radiolabeling of DOTA conjugate 1.

For electrospray ionization mass spectrometry (ESI-MS) analysis of compounds, ThermoFinnigan LCQ "Classic" ion trap LC-MS instrument was used (Stanford University Mass Spectrometry facility). Voyager-DE RP Biospectrometry instrument was used for matrix-assisted laser desorption/ionization time-of-flight (MALDI-TOF) mass spectrometry (Stanford University PAN facility).

Circular Dichroism Spectroscopy. Typical procedure for the preparation of **Cu-1−Cu-4** (for CD study) is as follows. Compound 1 (1.0 mg) was dissolved in NaOAc buffer (0.1 M, pH 5.5, 940 μL). To this was added 10 mM CuCl$_2$ (60 μL, approximately 2.0 mol equiv). The reaction mixture was incubated at room temperature overnight with gentle agitation. The reaction was monitored by analytical HPLC and stopped when the starting material (compound 1) was consumed. D-Salt polyacrylamide desalting column (Pierce, Rockford, IL, USA) was used to purify the crude product. The purification was carried out according to the manufacturer's instruction. The column fractions were monitored by measuring the absorbance at 220 nm using Nanodrop spectrophotometer. Fractions containing **Cu-1** were combined and lyophilized.

Circular dichroism measurements were carried out at 20 °C with a Jasco J-815 circular dichroism spectrometer (Jasco, Inc., Easton, MD, USA). CD spectra were obtained in an 1 mm path length quartz cell and recorded from 190 to 260 nm in 1 nm increments with a scanning speed of 20 nm/min and a response time of 4 s. Three scans for each sample were averaged. Sample concentrations were in 50 μM. Data are expressed in terms of per-residue molar ellipticity (deg cm^2/dmol) calculated per number of amides in a molecule.

Radiolabeling. DOTA-conjugated compounds (10 μg) were used for labeling. The bioconjugate was radiolabeled with ^{64}Cu by addition of ^{64}CuCl$_2$ (111 MBq, 3 mCi) in NaOAc buffer (pH 5.5, 0.1 N) followed by a 40 min incubation at 40 °C. EDTA (5 μL, 10 mM) was then added to quench free ^{64}Cu^{2+}. The radiolabeled complex was purified by analytical radio-HPLC. The mobile phase was used as follows: [A, water + 0.1% TFA; B, CH$_3$CN + 0.1% TFA] 3 min using 5% B, then a linear gradient to 65% B over 30 min, then going to 85% B over 3 min, maintaining this solvent composition for another 3 min, and then a linear gradient back to 5% B over 3 min (total 42 min). Flow rate of the radio-HPLC was 1.0 mL/min. Fractions containing pure radiolabeled peptoid (or peptide) were
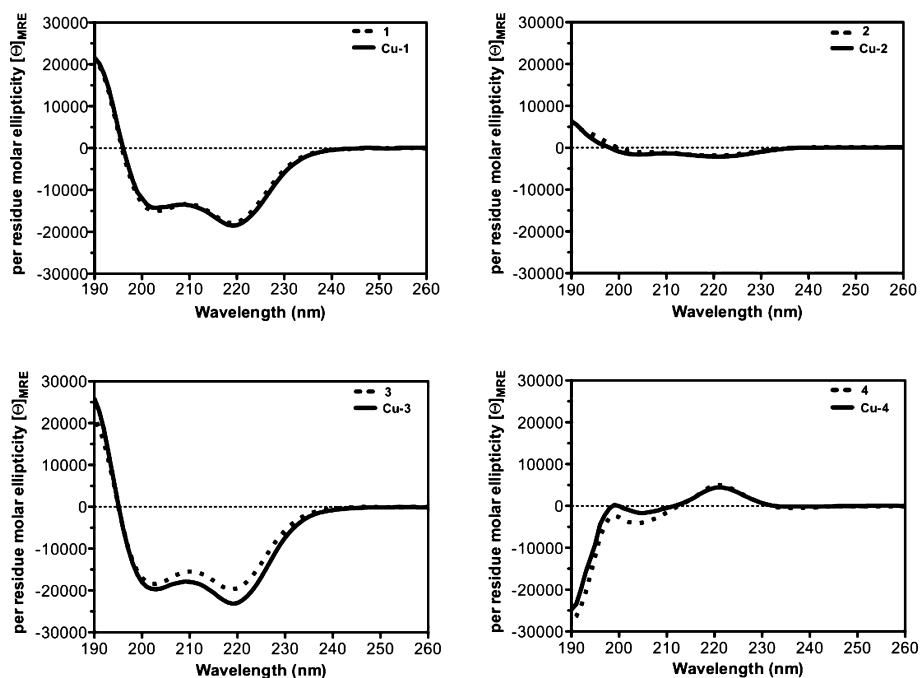
Figure 3. CD spectra of **1–4** and **Cu-1–Cu-4** in water (50 μM, 20 °C) were recorded as per-residue molar ellipticity (deg cm^2/dmol).

combined and dried under reduced pressure using rotary evaporator. The radiolabeled compound was reconstituted in phosphate-buffered saline (PBS) and passed through a 0.22 μm Millipore filter into a sterile vial for *in vitro* and animal experiments.

Biodistribution. ^{64}Cu-DOTA-peptoids or peptides (30–40 μCi) were injected into a tail vein in Balb/c mice ($n = 4$ for each group), and then the mice were sacrificed at 2 and 24 h p.i. For peptoid ^{64}**Cu-1**, three administration routes including intraperitoneal (i.p.), intravenous (i.v.) or gavages needle (p.o.) injection were used to compare the *in vivo* profiles of the peptoid. Major organs were excised and weighed, and their radioactivity was measured in a Wallac 1480 automated γ-counter (Perkin-Elmer, MA, USA). The radioactivity uptake in the organs was expressed as a percentage of the injected radioactive dose per gram of tissue (% ID/g).

Small Animal PET Imaging. Small animal PET imaging of Balb/c mice was performed on a microPET R4 rodent model scanner (Siemens Medical Solutions USA, Inc., Knoxville, TN, USA). The mice were injected with ^{64}Cu-DOTA-peptoids or peptides (~40 μCi) through the tail vein. A dynamic image of the first 35 min and a series of static images were acquired. During the scan, anesthesia was maintained with 2% isofluorane in 1 L/min oxygen, and imaging was performed in a prone position. For dynamic scan, image acquisition was initiated once the mice were centered in the field of view. Radiolabeled peptoid was administered with immediate data collection and image acquisition. Acquisition lasted about 35 min. Image reconstruction was performed by a two-dimensional OSEM (ordered subsets expectation maximum) algorithm with a spatial resolution of 1.66–1.85 mm. No attenuation or partial volume corrections were performed. Regions of interest (ROIs) were selected using ASIPro VM software (Siemens Medical Solutions USA Inc., Knoxville, TN, USA). For static scan at different times p.i. (0.25, 1, 2, 4, and 24 h), the mice were anesthetized with 2% isofluorane and placed in the prone position and in the center of the field of view of microPET. The 5 min static scans were

obtained, and the images were reconstructed by the OSEM algorithm. PET images were imported using ASIPro VM. ROIs were drawn manually over the organ of interest on decay-corrected whole-body coronal images. The mean counts per pixel per minute were obtained from the ROIs and converted to counts per milliliter per minute by using a calibration constant. No attenuation correction was performed.

Statistical Methods. Statistical analysis was performed using the Student's t-test for unpaired data. A 95% confidence level was chosen to determine the significance between groups, with $P < 0.05$ being significantly different.

■ RESULTS

Synthesis and Radiolabeling. Five DOTA conjugated compounds (three different cationic amphipathic peptoids **1–3** and two peptide controls **4–5** in Figure 1) were successfully synthesized by solid-phase synthesis followed by N-terminal DOTA conjugation. Both peptoid and peptide sequences were synthesized by automated peptide synthesizer according to the submonomer protocol[20] and standard Fmoc/tBu method,[54] respectively (Figure 2A). Then, the DOTA chelator was manually conjugated at the N-terminus of the pepoids or peptides by activating the carboxylic acid of DOTA-tris(t-Bu ester) with HATU (Figure 2B).[55] After deprotection and cleavage from the resin with trifluoroacetic acid, the DOTA conjugates were purified by preparative HPLC. It should be noted that less than 2 h of cleavage/deprotection resulted in incomplete *tert*-butyl ester deprotection of DOTA-tris(t-Bu ester); therefore, 2–3 h of cleavage reaction were used for all five compounds. The identity of each compound was confirmed by mass spectrometry (Supporting Information, Table S1).

Subsequently, the conjugates were radiolabeled with ^{64}Cu in order to monitor their *in vivo* behaviors (Figure 2C). The purification of radiolabeled complex, using a PD-10 column, afforded ^{64}Cu-DOTA-peptoid/peptide (^{64}**Cu-1**–^{64}**Cu-5**) with >95% radiochemical purity and modest specific activity of 3.98–6.83 MBq/nmol. Further mouse serum stability test

demonstrated that over 95% radiolabeled complexes remained intact after 1 h incubation at 37 °C (Supporting Information, Figure S5).

Circular Dichroism Studies. Conformational information of unmetalated **1**−**4** as well as copper-incorporated conjugates **Cu-1**−**Cu-4** was obtained by circular dichroism (CD) spectroscopy (Figure 3). CD study of pexiganan was previously reported (Table 1);[56] therefore, compound **5** was not included in this study. For the CD study, nonradioactive copper-bound DOTA conjugates, namely, **Cu-1**−**Cu-4**, was prepared, and the physicochemical properties of radioactive and nonradioactive copper compounds are assumed to be the same.

For helical peptoid conjugates **1** and **3**, the maintenance of helical folds was observed after copper incorporation (**Cu-1** and **Cu-3**). In addition, conformations of **1** and **Cu-1** at body temperature (37 °C) were examined and indicated minimal temperature dependence at 20 and 37 °C (Supporting Information, Figure S2). As predicted, compounds **2** and **Cu-2** indicated an almost unstructured conformation due to the lack of structure-inducing residue, Nspe or (S)-N-(1-phenylethyl)glycine, in the peptoid sequence. Uncharacteristic, but α-helix-like, CD signatures were obtained for **4** and **Cu-4**, and the handedness was the opposite of the peptoid conjugates' handedness. The CD spectra in this study clearly showed that the influence of copper incorporation on the overall conformation was minimal.

Biodistribution. Radiolabeled peptoids and peptides [64]Cu-1−[64]Cu-5 were injected intravenously into a tail vein in Balb/c mice. After 2 and 24 h postinjection (p.i.), the mice were euthanized, and the radioactivity of the organs and the blood was determined. The activity in the selected organs was expressed as a percentage of the injected radioactivity per gram of tissue (%ID/g). The results of the biodistribution studies are summarized in Figure 4.

Peptoid conjugates [64]Cu-1 and [64]Cu-2 exhibited prominent uptake in the liver, with lower liver uptake for [64]Cu-2 than [64]Cu-1. The detected activity in the liver was 137.6 ± 13.4%ID/g for [64]Cu-1 and 125.3 ± 16.8%ID/g for [64]Cu-2 at 2 h p.i., and the activity remained at 95.6 ± 10.5%ID/g for [64]Cu-1 and 72.2 ± 11.3%ID/g for [64]Cu-2 at 24 h p.i. Compared with [64]Cu-1 and ^{64}Cu-2, [64]Cu-3 exhibited lower liver uptake at both 2 and 24 h p.i. with 56.7 ± 1.8%ID/g and 47.3 ± 4.4%ID/g, respectively. Unlike the liver uptake, [64]Cu-3 showed the highest kidney uptake, which was around 31.2 ± 3.6%ID/g at 2 h, while it was 14.4 ± 0.9%ID/g and 12.55 ± 2.3%ID/g for [64]Cu-1 and ^{64}Cu-2, respectively. At 24 h p.i., the activity of [64]Cu-3 in the kidney remained 19.3 ± 2.6%ID/g, which was the highest level of all the conjugates tested in this study.

As for the peptide controls, both [64]Cu-4 and [64]Cu-5 showed lower liver uptake and faster liver clearances compared to all three peptoid conjugates ($P < 0.05$). [64]Cu-4 has a direct sequence homology to [64]Cu-1 and a similar hydrophobicity to [64]Cu-2 (Table 1). Compared to both peptides, [64]Cu-4 showed lower liver uptake and higher kidney uptake at 2 h p.i. (Figure 4A), reminiscent of the different hydrodynamic radii coming from the lack of hydrogen-bond donors in the peptoid backbone. Then, the kidney activity of [64]Cu-4 decreases faster and becomes similar to that of [64]Cu-2 at 24 h p.i. (Figure 4B), which can be explained by the higher in vivo stability of peptoids over peptides. Between the two peptides, less hydrophobic [64]Cu-5 exhibited lower liver uptake than [64]Cu-4 did. In addition, [64]Cu-5 had a much lower spleen uptake than the other four conjugates tested at both 2 and 24 h. All three peptoids and two peptides showed minimal brain uptake (lower
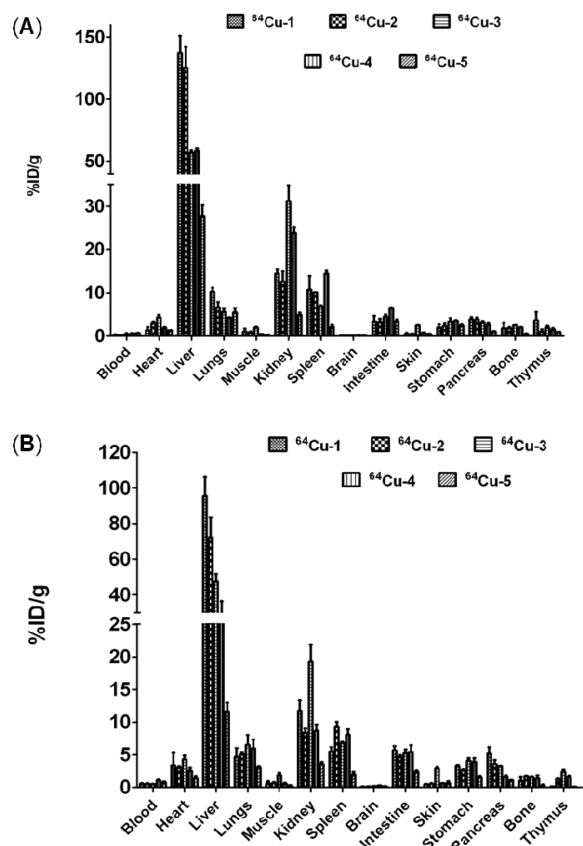

Figure 4. Biodistribution of ^{64}Cu-DOTA-peptoids/peptides ([64]Cu-1−[64]Cu-5) in Balb/c mice at 2 h (A) and 24 h (B). Data were expressed as mean ± SD, indicating the percentage administered activity (injected dose) per gram of tissue (%ID/g) after intravenous injection of about 40 μCi (1.48 MBq) tracers (n = 4).

than 1%ID/g), suggesting their incapability of crossing the blood-brain-barrier.

The effects of different administration routes (oral, intravenous, and intraperitoneal) on the in vivo biodistribution were then examined using [64]Cu-1 (Supporting Information, Figure S3). When administered intraperitoneally, predominant disposition of [64]Cu-1 was in the abdomen region. After intraperitoneal injection, activity was detected in most abdomen organs including intestine, colon, stomach, liver, spleen, and pancreas, and the activity persisted through 24 h. Significant kidney and thymus uptake was also observed after the intraperitoneal injection. When administered orally, the activity in stomach reached up to 4.82 ± 1.44%ID/g at 2 h and then dropped to 0.54 ± 0.22%ID/g at 24 h. The uptake of [64]Cu-1 could only be measured in the digestive system (i.e., stomach, small intestine, colon), suggesting that [64]Cu-1 cannot be absorbed into blood circulations when administered orally.

Small-Animal PET Imaging. Imaging studies were conducted at 0.25, 1, 2, 4, and 24 h after tail vein injection of [64]Cu-1−[64]Cu-5. Decay-corrected coronal microPET images are shown in Figure 5. Three peptoids and two peptides displayed different in vivo distribution patterns; particularly, uptakes in liver and in kidney were noticeable. For [64]Cu-1 and ^{64}Cu-2, the main excretion route is likely hepatic; little kidney activity was observed. [64]Cu-3 demonstrated the highest kidney activity of all three peptoids. Compared to peptides, higher kidney activity and lower liver activity were observed for peptides.
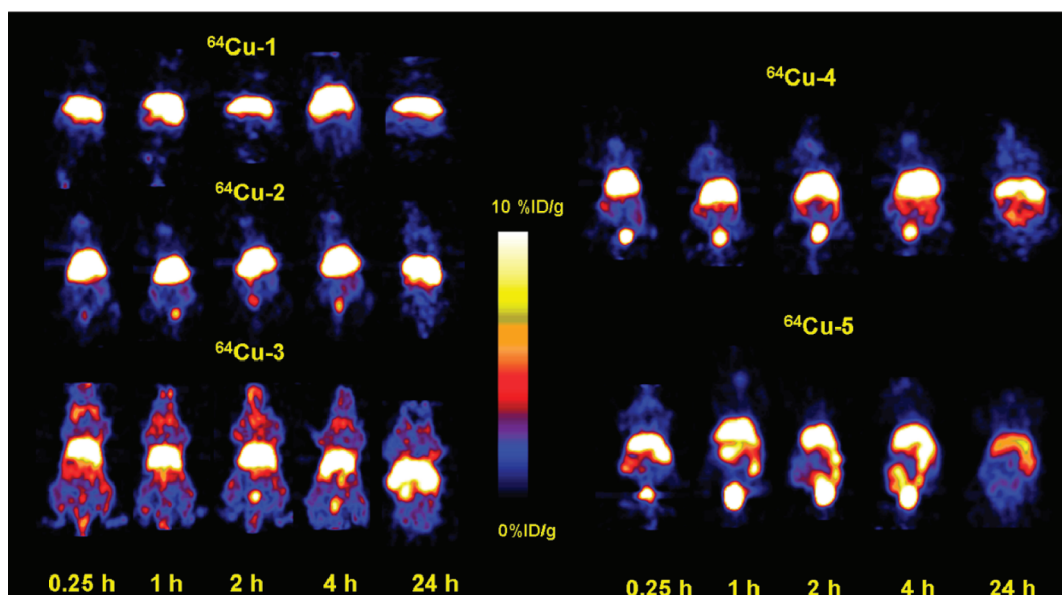
Figure 5. Representative decay-corrected coronal small-animal PET images of Balb/c mice at different time points after intravenous (iv) injection of ^{64}Cu-1−^{64}Cu-5 (n = 4 for each group).
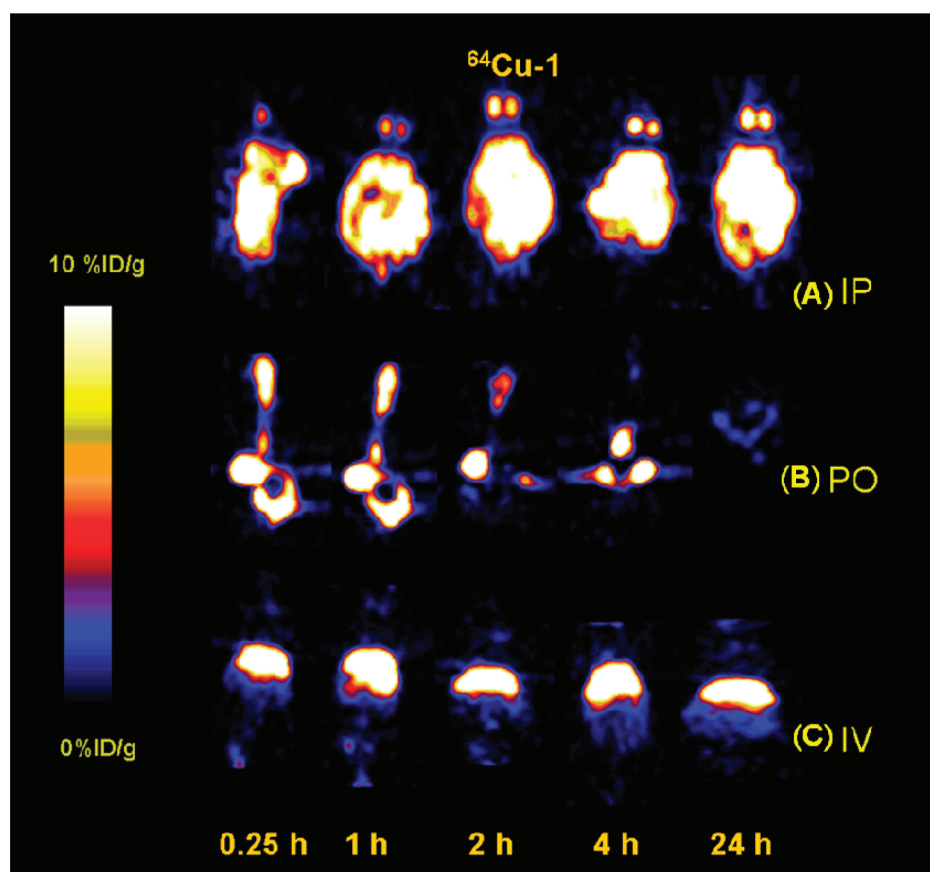

Figure 6. Representative decay-corrected coronal small-animal PET images of Balb/c mice at different time points after administration of ^{64}Cu-1 through peritoneal (A), oral (B), and intravenous (C) injections (n = 4 for each group).

Among the tested conjugates, ^{64}Cu-5 showed fastest clearance in both hepatic and renal pathways. Activity in the gastrointestinal (GI) tract could also be observed for all tested compounds, but markedly lower for ^{64}Cu-1.

The distribution patterns of ^{64}Cu-1 with different administration routes were compared and shown by PET imaging

(Figure 6). Radioactivity was found throughout the whole abdominal cavity when ^{64}Cu-1 was administered intraperitoneally. The permissive activity in abdomen clears rather slowly; therefore, it was complicated to differentiate organs in 24 h based upon PET imaging. Interestingly, a symmetrical anatomical structure was distinctly visible inside the upper body

of the mice after the intraperitoneal administration of ^{64}Cu-1, and biopsy confirmed the symmetrical organ as thymus. Thymic uptake has been reported for several radioactive pharmaceuticals such as ^{18}F-fluorodeoxyglucose (^{18}F-FDG), radioiodine, and gallium-67 citrate; however, the mechanism through which it occurs is not completely understood.[57,58] When ^{64}Cu-1 was administered through the tail vein, the compound essentially accumulated in the liver through 24 h as described above. Very low GI activity and kidney activity were observed in 24 h. In mice with orally administered ^{64}Cu-1, only GI activity was observed initially, and the peptoid conjugate was eliminated after 24 h as seen from PET imaging at 24 h p.i. A similar distribution pattern was observed for the oral administration of ^{64}Cu-3 (Supporting Information, Figure S4).

■ DISCUSSION

Designed to mimic naturally occurring proteins and peptides, peptoids are interesting materials whose properties lie in between natural biopolymers and non-natural synthetic polymers. The structural similarity to peptides enabled peptoids to exhibit an impressive diversity of biological activity;[28−30] however, the slight variation of backbone structure provides peptoids with distinct pharmacological properties such as resistance to proteolysis.[21−23]

Previously, a library of cationic amphipathic peptoids were synthesized based upon defined sequences and variations of secondary structures. It was demonstrated that the main chain length, helicity, charge, and hydrophobicity of peptoids could alter the *in vitro* antimicrobial activity.[31,32] Similarly, we envisioned that the modulation of peptoid structure could influence the *in vivo* pharmacokinetic profiles and biodistribution, which is critical information for further development of antimicrobial peptoids as therapeutic agents.

Previous *in vivo* data on biodistribution of peptoids are limited. Wang et al. used a ^{3}H-labeled tripeptoid to test the absorption and disposition in rats and compared the labeled tripeptoid to a ^{3}H-labeled tetrapeptide.[59] The tripeptoid appeared to be more metabolically stable, but showed lower oral absorption and more rapid biliary excretion. Although the *in vivo* pharmacokinetic properties of peptoid were investigated, the peptoids tested by Wang et al. can be classified as a small molecule with molecular weight less than 500 Da. In our present study, we examined antimicrobial peptoids that have secondary structures and molecular weight higher than 1500 Da, which render the peptoids similar to small proteins rather than to small molecules. Since distinct pharmacological properties between small and large molecules are reported,[60] biodistribution study of the antimicrobial peptoids is important for further *in vivo* applications.

When designing radiolabeled conjugates, we chose ^{64}Cu-DOTA labeling at the N-terminus of peptoids because we expected (1) more straightforward synthesis and (2) less impact on the peptoid secondary structure. The latter was confirmed by CD study. The comparison of CD spectra before and after N-terminal DOTA conjugation indicated nearly identical CD signatures: the intensity of spectral maxima at 190 nm and minima at 220 nm did not change much.[32] If the labeling was made on the side chain, the impact on the peptoid conformation could be larger. CD spectra in Figure 3 clearly demonstrate minimal conformational change after Cu^{2+} binding. Although our observation proves neither DOTA conjugation nor metalation changed the CD signature of peptoid, this does not prove that the peptoid with complexed Cu^{2+} has the same pharmacokinetic characteristics. Nonetheless,

the CD data prove useful as a preliminary indicator of intact peptoid conformation after radiolabeling.

The hepatobiliary system and the kidneys are the major routes by which drugs and their metabolites are eliminated from the body. Generally, small and hydrophilic organic compounds are preferentially excreted via the kidneys. In contrast, compounds with relatively high molecular weight (>500 Da) and amphipathic structure are mainly excreted via the liver (and then into bile).[60,61] As large and amphipathic compounds, ^{64}Cu-1−^{64}Cu-5 all showed that major uptake and excretion occurred in the liver; however, different uptake profiles in the liver and in the kidney are observed for each conjugate by the combined effect of the structure, hydrophobicity, and resistance to proteolysis (Figures 4 and 5).

After intravenous administration, biodistribution studies of ^{64}Cu-1 demonstrated highest liver accumulations at both 2 and 24 h (Figure 4). A slow elimination from the liver region was observed by PET images (Figure 5). Although the secondary structures of ^{64}Cu-1 and ^{64}Cu-2 are very distinct, they showed similar *in vivo* pharmacokinetics based on biodistribution and microPET studies, suggesting their overall hydrophobicity and amphipathicity. At both 2 and 24 h p.i., ^{64}Cu-3 showed the highest level of kidney uptake among all three peptoids and two peptides tested (Figure 4). With only one shorter hydrophobic residue than ^{64}Cu-1, ^{64}Cu-3 showed more than 50% lower liver uptake and noticeably higher kidney uptake; and this result exemplifies the strong influence of structural modification on *in vivo* biodistribution. Both biodistribution and PET results indicated faster clearance of peptide controls compared to peptoids (Figures 4 and 5). ^{64}Cu-5 indicated lowest uptake in both the liver and the kidney and fastest elimination. Along with the hydrophilic property of ^{64}Cu-5, the random coil structure, therefore vulnerability to proteolysis, can explain the result.

Different administration routes were investigated with ^{64}Cu-1 and ^{64}Cu-3. When administered orally, the peptoids showed poor bioavailability. The minimal absorption was indicated by high activity in the GI tract and little activity in the liver or in the kidney system (Supporting Information, Figure S3 and S4). For peptides, poor oral bioavailability has been widely accepted,[62] and our result suggests the similarity between peptides and peptoids in terms of the poor absorption after oral administration. However, it should be noted that peptides usually have rapid elimination kinetics in the range of minutes due to the extensive hydrolysis in the GI tract by peptidases.[63,64] Therefore, the 24 h passage through the GI tract without rapid digestion constitutes a unique aspect of peptoids, which originates from the protease resistance and the property as a non-natural biopolymer. The high *in vivo* stability of peptoids can be advantageous for some applications. If the site of action of a designed peptoid is in the GI tract, such as peptoid-based bacterial toxin sequestrants developed by Kodadek et al.[65] or antimicrobial peptoids for bacterial digestive infections, oral administration may provide a better therapeutic effect. Prolonged localized exposure to the pathogens and fewer side effects are expected due to the longer retention in the GI tract and the poor absorption to the systemic circulation, respectively.

Our data indicated that peptoids, compared to peptides, had a general *in vivo* property of higher tissue accumulation and slower elimination as well as higher stability. These observations can be rationalized in two ways: membrane permeability and protease resistance. Studies have shown that the cellular uptake could be improved by directly translating peptides into peptoids

due to the lipophilic nature and the stability of peptoids compared to those of peptides.[24,37,66] In addition, peptoids used in this study are cationic and amphipathic, which are recently found to be effective in cell membrane penetration.[44] As the first step for the tissue uptake is transport across the cell membrane (i.e., proximal tubular cells for the kidney uptake or hepatocyte cells for the liver uptake),[60,61] the efficient membrane permeability of the cationic amphipathic peptoids appears to play an important role in the higher tissue uptake. Second, the *in vivo* stability of peptoids against proteolysis provides longer circulation time, which leads to the higher tissue uptake and slower elimination.

Unique *in vivo* properties of cationic amphipathic peptoids are demonstrated in our study. Applications of the peptoids, for example, as a long-lasting liver targeting carrier or as an antimicrobial therapeutic agent against digestive infections or against urinary tract infections, now seem to be reasonable.

In conclusion, our results suggest that the *in vivo* pharmacokinetics of peptoids can be tuned by varying the structure and modifying the physicochemical properties of peptoids. In comparison to peptides, peptoids exhibited higher *in vivo* stability, higher tissue uptake, and a slower elimination rate. The *in vivo* biodistribution of peptoids can be confirmed by real-time small animal PET imaging. Using the noninvasive *in vivo* imaging approaches described here, pharmacokinetic properties of various peptoids can be predicted, which will provide useful information for suitable application and development of the peptoids.

■ ASSOCIATED CONTENT

Ⓢ Supporting Information

Supplementary figures and tables including HPLC, ESI-MS, CD spectra, biodistribution data, and PET images. This material is available free of charge via the Internet at http://pubs.acs.org.

■ AUTHOR INFORMATION

Corresponding Author

*Zhen Cheng, Ph.D.: 650-723-7866 (Phone), 650-736-7925 (Fax), E-mail: zcheng@stanford.edu. Annelise E. Barron, Ph.D.: 650-721-1151 (Phone), E-mail: aebarron@stanford.edu.

Author Contributions

#These authors contributed equally to this work.

Notes

The authors declare no competing financial interest.

■ ACKNOWLEDGMENTS

■ ABBREVIATIONS:

AMP, antimicrobial peptide; PET, positron emission tomography; CD, circular dichroism; MBq, megabecquerel; Ci, curie; I.P., intraperitoneal; I.V., intravenous; P.O., oral; P.I., postinjection; % ID/g, percentage of injected dose per gram of tissue; GI, gastrointestinal; DOTA, 1,4,7,10-tetraazacyclododecane-1,4,7,10-tetraacetic acid; TFA, trifluoroacetic acid; TIS, triisopropylsilane; HATU, 2-(7-aza-1*H*-benzotriazole-1-yl)-1,1,3,3-tetramethyluronium hexafluorophosphate; DIEA, *N,N*-diisopropylethylamine; DMF, *N,N*-dimethylformamide; Nspe,

(S)-*N*-(1-phenylethyl)glycine; MIC, minimum inhibitory concentration

■ REFERENCES

(1) Hancock, R. E. W., and Sahl, H. G. (2006) Antimicrobial and host-defense peptides as new anti-infective therapeutic strategies. *Nat. Biotechnol.* 24, 1551−1557.

(2) Mygind, P. H., Fischer, R. L., Schnorr, K. M., Hansen, M. T., Sonksen, C. P., Ludvigsen, S., Raventos, D., Buskov, S., Christensen, B., De Maria, L., Taboureau, O., Yaver, D., Elvig-Jorgensen, S. G., Sorensen, M. V., Christensen, B. E., Kjaerulff, S., Frimodt-Moller, N., Lehrer, R. I., Zasloff, M., and Kristensen, H. H. (2005) Plectasin is a peptide antibiotic with therapeutic potential from a saprophytic fungus. *Nature 437*, 975−980.

(3) Brown, K. L., and Hancock, R. E. W. (2006) Cationic host defense (antimicrobial) peptides. *Curr. Opin. Immunol. 18*, 24−30.

(4) Zasloff, M. (1992) Antibiotic peptides as mediators of innate immunity. *Curr. Opin. Immunol. 4*, 3−7.

(5) Hamill, P., Brown, K., Jenssen, H., and Hancock, R. E. (2008) Novel anti-infectives: is host defence the answer? *Curr. Opin. Biotechnol. 19*, 628−636.

(6) Scott, M. G., Dullaghan, E., Mookherjee, N., Glavas, N., Waldbrook, M., Thompson, A., Wang, A., Lee, K., Doria, S., Hamill, P., Yu, J. J., Li, Y., Donini, O., Guarna, M. M., Finlay, B. B., North, J. R., and Hancock, R. E. (2007) An anti-infective peptide that selectively modulates the innate immune response. *Nat. Biotechnol. 25*, 465−472.

(7) Nolan, E. M., and Walsh, C. T. (2009) How nature morphs peptide scaffolds into antibiotics. *ChemBioChem 10*, 34−53.

(8) Marr, A. K., Gooderham, W. J., and Hancock, R. E. (2006) Antibacterial peptides for therapeutic use: obstacles and realistic outlook. *Curr. Opin. Pharmacol. 6*, 468−472.

(9) Radzishevsky, I. S., Rotem, S., Zaknoon, F., Gaidukov, L., Dagan, A., and Mor, A. (2005) Effects of acyl versus aminoacyl conjugation on the properties of antimicrobial peptides. *Antimicrob. Agents Chemother. 49*, 2412−2420.

(10) Scott, R. W., DeGrado, W. F., and Tew, G. N. (2008) De novo designed synthetic mimics of antimicrobial peptides. *Curr. Opin. Biotechnol. 19*, 620−627.

(11) Vagner, J., Qu, H., and Hruby, V. J. (2008) Peptidomimetics, a synthetic tool of drug discovery. *Curr. Opin. Chem. Biol. 12*, 292−296.

(12) Thayer, A. M. (2011) Improving peptides. *Chem. Eng. News 89*, 13−20.

(13) Radzishevsky, I. S., Rotem, S., Bourdetsky, D., Navon-Venezia, S., Carmeli, Y., and Mor, A. (2007) Improved antimicrobial peptides based on acyl-lysine oligomers. *Nat. Biotechnol. 25*, 657−659.

(14) Liu, D., and DeGrado, W. F. (2001) De novo design, synthesis, and characterization of antimicrobial beta-peptides. *J. Am. Chem. Soc. 123*, 7553−7559.

(15) Porter, E. A., Weisblum, B., and Gellman, S. H. (2002) Mimicry of host-defense peptides by unnatural oligomers: antimicrobial beta-peptides. *J. Am. Chem. Soc. 124*, 7324−7330.

(16) Fernandez-Lopez, S., Kim, H. S., Choi, E. C., Delgado, M., Granja, J. R., Khasanov, A., Kraehenbuehl, K., Long, G., Weinberger, D. A., Wilcoxen, K. M., and Ghadiri, M. R. (2001) Antibacterial agents based on the cyclic D,L-alpha-peptide architecture. *Nature 412*, 452−455.

(17) Srinivas, N., Jetter, P., Ueberbacher, B. J., Werneburg, M., Zerbe, K., Steinmann, J., Van der Meijden, B., Bernardini, F., Lederer, A., Dias, R. L., Misson, P. E., Henze, H., Zumbrunn, J., Gombert, F. O., Obrecht, D., Hunziker, P., Schauer, S., Ziegler, U., Kach, A., Eberl, L., Riedel, K., DeMarco, S. J., and Robinson, J. A. (2010) Peptidomimetic antibiotics target outer-membrane biogenesis in Pseudomonas aeruginosa. *Science 327*, 1010−1013.

(18) Goodson, B., Ehrhardt, A., Ng, S., Nuss, J., Johnson, K., Giedlin, M., Yamamoto, R., Moos, W. H., Krebber, A., Ladner, M., Giacona, M. B., Vitt, C., and Winter, J. (1999) Characterization of novel antimicrobial peptoids. *Antimicrob. Agents Chemother. 43*, 1429−1434.

(19) Simon, R. J., Kania, R. S., Zuckermann, R. N., Huebner, V. D., Jewell, D. A., Banville, S., Ng, S., Wang, L., Rosenberg, S., Marlowe, C.

K., et al. (1992) Peptoids: a modular approach to drug discovery. *Proc. Natl. Acad. Sci. U.S.A. 89,* 9367−9371.

(20) Zuckermann, R. N., Kerr, J. M., Kent, S. B. H., and Moos, W. H. (1992) Efficient method for the preparation of peptoids [oligo(N-substituted glycines)] by submonomer solid-phase synthesis. *J. Am. Chem. Soc. 114,* 10646−10647.

(21) Miller, S. M., Simon, R. J., Ng, S., Zuckermann, R. N., Kerr, J. M., and Moos, W. H. (1995) Comparison of the proteolytic susceptibilities of homologous L-amino acid, D-amino acid, and N-substituted clycine peptide and peptoid oligomers. *Drug Dev. Res. 35,* 20−32.

(22) Miller, S. M., Simon, R. J., Ng, S., Zuckermann, R. N., Kerr, J. M., and Moos, W. H. (1994) Proteolytic studies of homologous peptide and N-substituted glycine peptoid oligomers. *Bioorg. Med. Chem. Lett. 4,* 2657−2662.

(23) Kwon, Y. U., and Kodadek, T. (2007) Quantitative evaluation of the relative cell permeability of peptoids and peptides. *J. Am. Chem. Soc. 129,* 1508−1509.

(24) Tan, N. C., Yu, P., Kwon, Y. U., and Kodadek, T. (2008) High-throughput evaluation of relative cell permeability between peptoids and peptides. *Bioorg. Med. Chem. 16,* 5853−5861.

(25) Udugamasooriya, D. G., Dineen, S. P., Brekken, R. A., and Kodadek, T. (2008) A peptoid "antibody surrogate" that antagonizes VEGF receptor 2 activity. *J. Am. Chem. Soc. 130,* 5744−5752.

(26) Astle, J. M., Udugamasooriya, D. G., Smallshaw, J. E., and Kodadek, T. (2008) A VEGFR2 antagonist and other peptoids evade immune recognition. *Int. J. Pept. Res. Ther. 14,* 223−227.

(27) Fowler, S. A., and Blackwell, H. E. (2009) Structure-function relationships in peptoids: recent advances toward deciphering the structural requirements for biological function. *Org. Biomol. Chem. 7,* 1508−1524.

(28) Yoo, B., and Kirshenbaum, K. (2008) Peptoid architectures: elaboration, actuation, and application. *Curr. Opin. Chem. Biol. 12,* 714−721.

(29) Zuckermann, R. N., and Kodadek, T. (2009) Peptoids as potential therapeutics. *Curr. Opin. Mol. Ther. 11,* 299−307.

(30) Seo, J., Lee, B.-C., and Zuckermann, R. N. (2011) Peptoids: synthesis, characterization and nanostructures, in *Comprehensive Biomaterials* (Ducheyne, P., Healy, K. E., Hutmacher, D. W., Grainger, D. W., and Kirkpatric, C. J., Ed.) pp 53−76, Elsevier.

(31) Patch, J. A., and Barron, A. E. (2003) Helical peptoid mimics of magainin-2 amide. *J. Am. Chem. Soc. 125,* 12092−12093.

(32) Chongsiriwatana, N. P., Patch, J. A., Czyzewski, A. M., Dohm, M. T., Ivankin, A., Gidalevitz, D., Zuckermann, R. N., and Barron, A. E. (2008) Peptoids that mimic the structure, function, and mechanism of helical antimicrobial peptides. *Proc. Natl. Acad. Sci. U.S.A. 105,* 2794−2799.

(33) Chongsiriwatana, N. P., Miller, T. M., Wetzler, M., Vakulenko, S., Karlsson, A. J., Palecek, S. P., Mobashery, S., and Barron, A. E. (2011) Short alkylated peptoid mimics of antimicrobial lipopeptides. *Antimicrob. Agents Chemother. 55,* 417−420.

(34) Chongsiriwatana, N. P., Wetzler, M., and Barron, A. E. (2011) Functional synergy between antimicrobial peptoids and peptides against gram-negative bacteria. *Antimicrob. Agents Chemother. 55,* 5399−5402.

(35) Kapoor, R., Wadman, M. W., Dohm, M. T., Czyzewski, A. M., Spormann, A. M., and Barron, A. E. (2011) Antimicrobial peptoids are effective against pseudomonas aeruginosa biofilms. *Antimicrob. Agents Chemother. 55,* 3054−3057.

(36) Kapoor, R., Eimerman, P. R., Hardy, J. W., Cirillo, J. D., Contag, C. H., and Barron, A. E. (2011) Efficacy of antimicrobial peptoids against mycobacterium tuberculosis. *Antimicrob. Agents Chemother. 55,* 3058−3062.

(37) Schroder, T., Niemeier, N., Afonin, S., Ulrich, A. S., Krug, H. F., and Brase, S. (2008) Peptoidic amino- and guanidinium-carrier systems: targeted drug delivery into the cell cytosol or the nucleus. *J. Med. Chem. 51,* 376−379.

(38) Wu, C. W., Sanborn, T. J., Huang, K., Zuckermann, R. N., and Barron, A. E. (2001) Peptoid oligomers with alpha-chiral, aromatic

side chains: Sequence requirements for the formation of stable peptoid helices. *J. Am. Chem. Soc. 123,* 6778−6784.

(39) Sanborn, T. J., Wu, C. W., Zuckermann, R. N., and Barron, A. E. (2002) Extreme stability of helices formed by water-soluble poly-N-substituted glycines (polypeptoids) with alpha-chiral side chains. *Biopolymers 63,* 12−20.

(40) Armand, P., Kirshenbaum, K., Falicov, A., Dunbrack, R. L., Jr., Dill, K. A., Zuckermann, R. N., and Cohen, F. E. (1997) Chiral N-substituted glycines can form stable helical conformations. *Fold. Des. 2,* 369−375.

(41) Kirshenbaum, K., Barron, A. E., Goldsmith, R. A., Armand, P., Bradley, E. K., Truong, K. T., Dill, K. A., Cohen, F. E., and Zuckermann, R. N. (1998) Sequence-specific polypeptoids: a diverse family of heteropolymers with stable secondary structure. *Proc. Natl. Acad. Sci. U.S.A. 95,* 4303−4308.

(42) Wu, C. W., Kirshenbaum, K., Sanborn, T. J., Patch, J. A., Huang, K., Dill, K. A., Zuckermann, R. N., and Barron, A. E. (2003) Structural and spectroscopic studies of peptoid oligomers with alpha-chiral aliphatic side chains. *J. Am. Chem. Soc. 125,* 13525−13530.

(43) Armand, P., Kirshenbaum, K., Goldsmith, R. A., Farr-Jones, S., Barron, A. E., Truong, K. T., Dill, K. A., Mierke, D. F., Cohen, F. E., Zuckermann, R. N., and Bradley, E. K. (1998) NMR determination of the major solution conformation of a peptoid pentamer with chiral side chains. *Proc. Natl. Acad. Sci. U.S.A. 95,* 4309−4314.

(44) Huang, W., Seo, J., Willingham, S. B., Czyzewski, A. M., Gonzalgo, M. L., Weissman, I. L., and Barron, A. E. unpublished results.

(45) Akhtar, M. S., Qaisar, A., Irfanullah, J., Iqbal, J., Khan, B., Jehangir, M., Nadeem, M. A., Khan, M. A., Afzal, M. S., ul-Haq, I., and Imran, M. B. (2005) Antimicrobial peptide Tc-99m-ubiquicidin 29−41 as human infection-imaging agent: Clinical trial. *J. Nucl. Med. 46,* 567−573.

(46) Brouwer, C. P. J. M., Wulferink, M., and Welling, M. M. (2008) The pharmacology of radiolabeled cationic antimicrobial peptides. *J. Pharm. Sci. 97,* 1633−1651.

(47) Ge, Y., MacDonald, D. L., Holroyd, K. J., Thornsberry, C., Wexler, H., and Zasloff, M. (1999) In vitro antibacterial properties of pexiganan, an analog of magainin. *Antimicrob. Agents Chemother. 43,* 782−788.

(48) Gottler, L. M., and Ramamoorthy, A. (2009) Structure, membrane orientation, mechanism, and function of pexiganan--a highly potent antimicrobial peptide designed from magainin. *Biochim. Biophys. Acta 1788,* 1680−1686.

(49) Lipsky, B. A., Holroyd, K. J., and Zasloff, M. (2008) Topical versus systemic antimicrobial therapy for treating mildly infected diabetic foot ulcers: a randomized, controlled, double-blinded, multicenter trial of pexiganan cream. *Clin. Infect. Dis. 47,* 1537−1545.

(50) Ametamey, S. M., Honer, M., and Schubiger, P. A. (2008) Molecular imaging with PET. *Chem. Rev. 108,* 1501−1516.

(51) Miao, Z., Ren, G., Liu, H., Jiang, L., and Cheng, Z. (2010) Small-animal PET imaging of human epidermal growth factor receptor positive tumor with a 64Cu labeled affibody protein. *Bioconjugate Chem. 21,* 947−954.

(52) Cheng, Z., Xiong, Z., Subbarayan, M., Chen, X., and Gambhir, S. S. (2007) 64Cu-labeled alpha-melanocyte-stimulating hormone analog for microPET imaging of melanocortin 1 receptor expression. *Bioconjugate Chem. 18,* 765−772.

(53) Burkoth, T. S., Fafarman, A. T., Charych, D. H., Connolly, M. D., and Zuckermann, R. N. (2003) Incorporation of unprotected heterocyclic side chains into peptoid oligomers via solid-phase submonomer synthesis. *J. Am. Chem. Soc. 125,* 8841−8845.

(54) Montalbetti, C. A. G. N., and Falque, V. (2005) Amide bond formation and peptide coupling. *Tetrahedron 61,* 10827−10852.

(55) Cheng, Z., Chen, J. Q., Miao, Y., Owen, N. K., Quinn, T. P., and Jurisson, S. S. (2002) Modification of the structure of a metal-lopeptide: Synthesis and biological evaluation of (111)in-labeled DOTA-conjugated rhenium-cyclized alpha-MSH analogues. *J. Med. Chem. 45,* 4588−4588.

(56) Ramamoorthy, A., Thennarasu, S., Lee, D. K., Tan, A., and Maloy, L. (2006) Solid-state NMR investigation of the membrane-disrupting mechanism of antimicrobial peptides MSI-78 and MSI-594 derived from magainin 2 and melittin. *Biophys. J. 91*, 206−216.

(57) Mello, M. E., Flamini, R. C., Corbo, R., and Mamede, M. (2009) Radioiodine concentration by the thymus in differentiated thyroid carcinoma: report of five cases. *Arq. Bras. Endocrinol. Metabol. 53*, 874−879.

(58) Connolly, L. P., and Connolly, S. A. (2003) Thymic uptake of radiopharmaceuticals. *Clin. Nucl. Med. 28*, 648−651.

(59) Wang, Y., Lin, H., Tullman, R., Jewell, C. F., Jr., Weetall, M. L., and Tse, F. L. (1999) Absorption and disposition of a tripeptoid and a tetrapeptide in the rat. *Biopharm. Drug Dispos. 20*, 69−75.

(60) Hagenbuch, B. (2010) Drug uptake systems in liver and kidney: a historic perspective. *Clin. Pharmacol. Ther. 87*, 39−47.

(61) van Montfoort, J. E., Hagenbuch, B., Groothuis, G. M., Koepsell, H., Meier, P. J., and Meijer, D. K. (2003) Drug uptake systems in liver and kidney. *Curr. Drug Metab. 4*, 185−211.

(62) Silverman, R. B. (2004) *The Organic Chemistry of Drug Design and Drug Action*, 2nd ed., Elsevier Academic Press, USA.

(63) Foltz, M., van der Pijl, P. C., and Duchateau, G. S. (2010) Current in vitro testing of bioactive peptides is not valuable. *J. Nutr. 140*, 117−118.

(64) Lee, H. J. (2002) Protein drug oral delivery: the recent progress. *Arch. Pharm. Res. 25*, 572−584.

(65) Simpson, L. S., Burdine, L., Dutta, A. K., Feranchak, A. P., and Kodadek, T. (2009) Selective toxin sequestrants for the treatment of bacterial infections. *J. Am. Chem. Soc. 131*, 5760−5762.

(66) Wender, P. A., Mitchell, D. J., Pattabiraman, K., Pelkey, E. T., Steinman, L., and Rothbard, J. B. (2000) The design, synthesis, and evaluation of molecules that enable or enhance cellular uptake: peptoid molecular transporters. *Proc. Natl. Acad. Sci. U.S.A. 97*, 13003−13008.